Renal clear cell sarcoma in children: A case report

LINGFEI LI[1*], HUI YANG[1*], FANG LI[1], NING ZHOU[1], YING LUO[1], HAILAN MA[1], ZHENGFU WANG[1], LIREN JIAN[1], LING DANG[2] and HONGYAN XIAO[1]

[1]Department of Pathology, Peking University First Hospital Ningxia Women and Children's Hospital (Ningxia Hui Autonomous Region Maternal and Child Health Hospital), Yinchuan, Ningxia 75004, P.R. China; [2]School of Nursing, Ningxia Medical University, Yinchuan, Ningxia 75004, P.R. China

Received November 7, 2025; Accepted March 13, 2026

DOI: 10.3892/br.2026.2159

Abstract. Clear cell sarcoma of the kidney (CCSK), a rare renal interstitial tumor in children, poses a notable threat to the physical and mental health of children because of its highly aggressive nature, tendency to compress surrounding tissue and potential for metastasis. The present study reports two cases of pediatric CCSK treated at the Peking University First Hospital Ningxia Women and Children's Hospital (Ningxia Hui Autonomous Region Maternal and Child Health Hospital, Ningxia, China; July 2024-2025.7). Both patients were female infants aged 1 year. Upon initial admission, they were misdiagnosed with nephroblastoma and received radical nephrectomy and vincristine chemotherapy. Pathological consultation and advanced molecular sequencing identified specific expression of the BCL6 corepressor gene in patient tumor tissue, leading to a definitive diagnosis of CCSK. Furthermore, the present study aimed to provide an overview of the aberrant genes associated with CCSK to provide a useful reference for future research on the pathogenesis of CCSK and improvement of molecular pathology.

Introduction

Clear cell sarcoma of the kidney (CCSK) is a rare and highly aggressive malignant tumor of the kidney that primarily affects infants and young children (1). CCSK accounts for 3-5% of childhood malignant renal tumors, making it rare among kidney cancers. Its incidence is higher in children aged <5 years, with a male-to-female ratio of ~2:1, showing a slight male predisposition for unknown reasons (2-4). The tumor typically originates from the mesenchymal tissue of the kidney and is located primarily in the renal medulla (the innermost part of the kidney), without a capsule and with focal boundaries, which make it difficult to distinguish from the surrounding tissues during surgery (5). Upon gross examination, the tumor surface typically appears tan and has a texture similar to that of fish flesh (2,5), a characteristic that aids identification during pathological analysis. Additionally, most tumors tend to be relatively large at the time of diagnosis, which may increase the complexity of surgical resection and affect the overall prognosis of patients. Clinically, patients with CCSK typically present with a palpable abdominal mass (6). CCSK can develop into bone and brain metastases relatively quickly (7). The aggressive behavior of this tumor typically results in poor prognosis, even with aggressive therapeutic interventions.

A combination of surgery and radiotherapy has been used to treat CCSK (8-10). However, the landscape of CCSK management has evolved with the introduction of chemotherapy. Chemotherapy protocols, especially those incorporating anthracycline drugs, have demonstrated encouraging outcomes, significantly increasing the 5-year survival rate to ~86% (11,12). These advancements highlight the growing role of chemotherapy in the multidisciplinary treatment of CCSK. Despite these promising findings, the literature on CCSK remains limited, reflecting a gap in understanding of this rare tumor (13). Further research is imperative not only to elucidate its pathogenesis but also to explore innovative and alternative treatment options. The present study reports two cases of CCSK observed at the Peking University First Hospital Ningxia Women and Children's Hospital (Ningxia Hui Autonomous Region Maternal and Child Health Hospital, Ningxia, China) and aimed to highlight the diagnostic challenges, particularly in promptly and accurately performing pathology in the context of CCSK, where the subtleties of tumor biology serve crucial roles.

Case report

The present study assessed two cases of CCSK in female patients aged 1 year who visited Peking University First Hospital Ningxia Women and Children's Hospital (Ningxia

Correspondence to: Dr Hongyan Xiao, Department of Pathology, Peking University First Hospital Ningxia Women and Children's Hospital (Ningxia Hui Autonomous Region Maternal and Child Health Hospital), 127 Hupian Road, Jinfeng, Yinchuan, Ningxia 75004, P.R. China
E-mail: xiaohongyan@nxfeyy.com

Professor Ling Dang, School of Nursing, Ningxia Medical University, 1160 Shengli Street, Xingqing, Yinchuan, Ningxia 75004, P.R. China
E-mail: 13995299070@163.com

*Contributed equally

Key words: clear cell sarcoma of the kidney, kidney tumor, case report, children

Hui Autonomous Region Maternal and Child Health Hospital) in December 2024. Clinical demographic data were obtained from medical records, referring doctors and subsequent telephone follow-up. The tumor samples were fixed, paraffin-embedded and stained with hematoxylin and eosin. Immunohistochemistry (IHC) was performed using the EnVision two-step method and all antibodies (Table SI) were used as positive controls. The high-throughput sequencing was completed at the Darui Diag Laboratory (Guangzhou) Co. For PCR-capillary electrophoresis sample processing, the sample was cut into sections measuring 5-10 μm. A total of 1 ml of xylene was added. The lid was closed, and the mixture was centrifuged at 6,000 x g speed for 2 min at room temperature. The supernatant was then removed by pipetting. Another 1 ml of xylene was added, followed by vortexing, and the process of centrifugation at 6,000 x g 23˚C and supernatant removal was repeated. After dewaxing, 1 ml of 96-100% ethanol was added to the pellet, which was then vortexed to mix and centrifuged at 6,000 x g speed for 2 min at room temperature. The lid was opened, and the sample was incubated at 15-25˚C for 10 min. The dried pellet was resuspended in 200 μl of Buffer GA, and 20 μl of Proteinase K was added. After vortexing, it was incubated at 56˚C for 1 h and then at 90˚C for 1 h. After lysis, 220 μl of Buffer GB was added, and the mixture was vortexed thoroughly. Then, 250 μl 96-100% ethanol was added, and it was vortexed again. The entire lysate was centrifuged at 6,000 x g and 23˚C for 2 min. A total of 500 μl of Buffer GD was added and centrifuged at 6,000 x g 23˚C for 1 min. Finally, 30-100 μl of ddH2O was added to the membrane center. The collected DNA was stored at -20˚C.

The inclusion criteria as follows: i) Age range. The age at diagnosis was ≤18 years (for children and adolescents), with a focus on the high-incidence age group of 1-6 years (accounting for over 80% of cases). 2. Pathological confirmation. The postoperative pathological specimens were reviewed by senior pathologists, and they met the diagnostic criteria of CCSK (homogeneous small round to oval cells, transparent or eosinophilic cytoplasm, prominent nucleoli, accompanied by dendritic fibrovascular septa. Immunohistochemistry: Vimentin and Cyclin D1 are positive, WT1 is negative; BCOR or YWHAE-NUTM2 gene fusion detection is positive (such as FISH, RT-PCR or NGS). Internal tandem duplication (ITD) of BCOR exon 15 or YWHAE::NUTM2 gene fusion (ideal diagnostic criteria); preoperative imaging (ultrasound, CT/MRI) showed renal space-occupying lesions, which were consistent with the typical manifestations of CCSK: Clear boundaries or slightly invasive, non-uniform enhancement on enhanced scanning. In the late stage, it could invade the renal vein, inferior vena cava or adjacent organs. Bone scan or PET-CT indicated bone metastasis (the CCSK bone metastasis rate is as high as 29%). by searching the hospital medical record system, pathological management system and relevant materials from other hospital consultations. The case collection process followed the requirements of the CARE guidelines (14) to ensure the completeness and accuracy of the case information.

The present study was approved (approval no. KJ-LL-2025004) by Peking University First Hospital Ningxia Women and Children's Hospital (Ningxia Hui Autonomous Region Maternal and Child Health Hospital). All methods were performed following the relevant guidelines and regulations. Informed consent was obtained from legal guardians of the patients.

Patient 1 was admitted in February 2024 following the discovery of an abdominal mass 3 days previously. A mass of ~11x6 cm in size could be palpated in the right abdomen. Color Doppler ultrasound revealed a solid mass in the right kidney, protruding into the abdominal cavity, ~13.9x7.7x8.9 cm in size, with rich blood flow inside (Fig. 1A and B). The patient was misdiagnosed with nephroblastoma and received two rounds of chemotherapy. The patient underwent right nephrectomy combined with retroperitoneal lymph node biopsy. The patient recovered well postoperatively. Histopathology revealed that the tumor cells were diffusely distributed, with vacuolated nuclei, pathological mitotic figures, rich blood vessels and extensive necrosis in certain areas. The tumor showed classic CCSK features, including chicken foot-like vascular septa partitioning cells into nests or cords. Tumor cell nuclei had fine granular chromatin, inconspicuous nucleoli, abundant clear cytoplasm and spoke-like arrangement (Fig. 1C-E). In certain areas, cells were whorled, presenting diverse morphology. IHC results (Fig. 1F-J) were as follows: Paired box gene 2 (PAX-2; +), cyclin D1 (+), BCOR (+): BCL6 Corepressor, CD99 (+): BCL-2 (+), TLE1 (+): transducin-like Enhancer Protein (TLE)1, SATB2 (+): Special AT-rich sequence-binding protein 2, S-100 (-), INI-1 (+): Integrase Interactor 1, WT1 (-): Wilms Tumor 1, Ki67 (40%+), CD56 (+) and vimentin (+), providing a diagnostic basis for CCSK.

Patient 2 was a 1-year-old female. The family noticed that urine flow was interrupted for 6 months and a mass of ~10x6 cm could be felt in the right abdomen. A CT scan of the pelvic and abdominal cavity revealed a cystic and solid mass ~9.7x8.9 cm in size in the middle and lower right kidney. Color Doppler ultrasound confirmed that the solid mass in the middle and lower pole of the right kidney was ~9.7x8.5x8.0 cm, and a nodule ~2.2x2.1x2.1 cm in size was found at the lower edge of the left part of the mass, with rich blood flow (Fig. 2A and B). The patient underwent surgery for nephroblastoma and received 4 weeks of chemotherapy as follows Vincristine 0.05 mg/kg, Cyclophosphamide 14.7 mg/kg per day for 3 days, Etoposide 3.3 mg/kg per day for 5 days. Each course lasts for 3-4 weeks. The histological features were more typical, with tumor cells of relatively uniform size, pale cytoplasm, fine nuclear chromatin, indistinct nucleoli and sheet-like distribution separated by branching fibrovascular stroma (Fig. 2C-E). The initial diagnosis was mesenchymal nephroblastoma, but IHC results [cyclin D1 (+), BCOR (+), CD99 (+), BCL-2 (+), TLE1 (+), SATB2 (-), S-100 (-), INI-1 (+), WT1 (-), Ki67 (40% positive staining), CD56 (+), PAX-2 (+), Brg1 (+); Fig. 2F-J] were consistent with clear cell sarcoma of the right kidney. Fluorescence *in situ* hybridization of the BCOR gene in the patient revealed a positive-staining cell percentage of 0% and no breakage or translocation of the BCOR gene. For PCR-capillary electrophoresis sample processing, excess paraffin had first been trimmed off the sample block with a scalpel, sections (5-10 μm thick) cut. The sections had been immediately placed in a 1.5 or 2 ml microcentrifuge tube, 1 ml xylene added, the lid closed, and the tube vortexed for 10 sec before centrifugation at 6,000 x g for 2 min at room temperature; the supernatant had been removed by pipetting

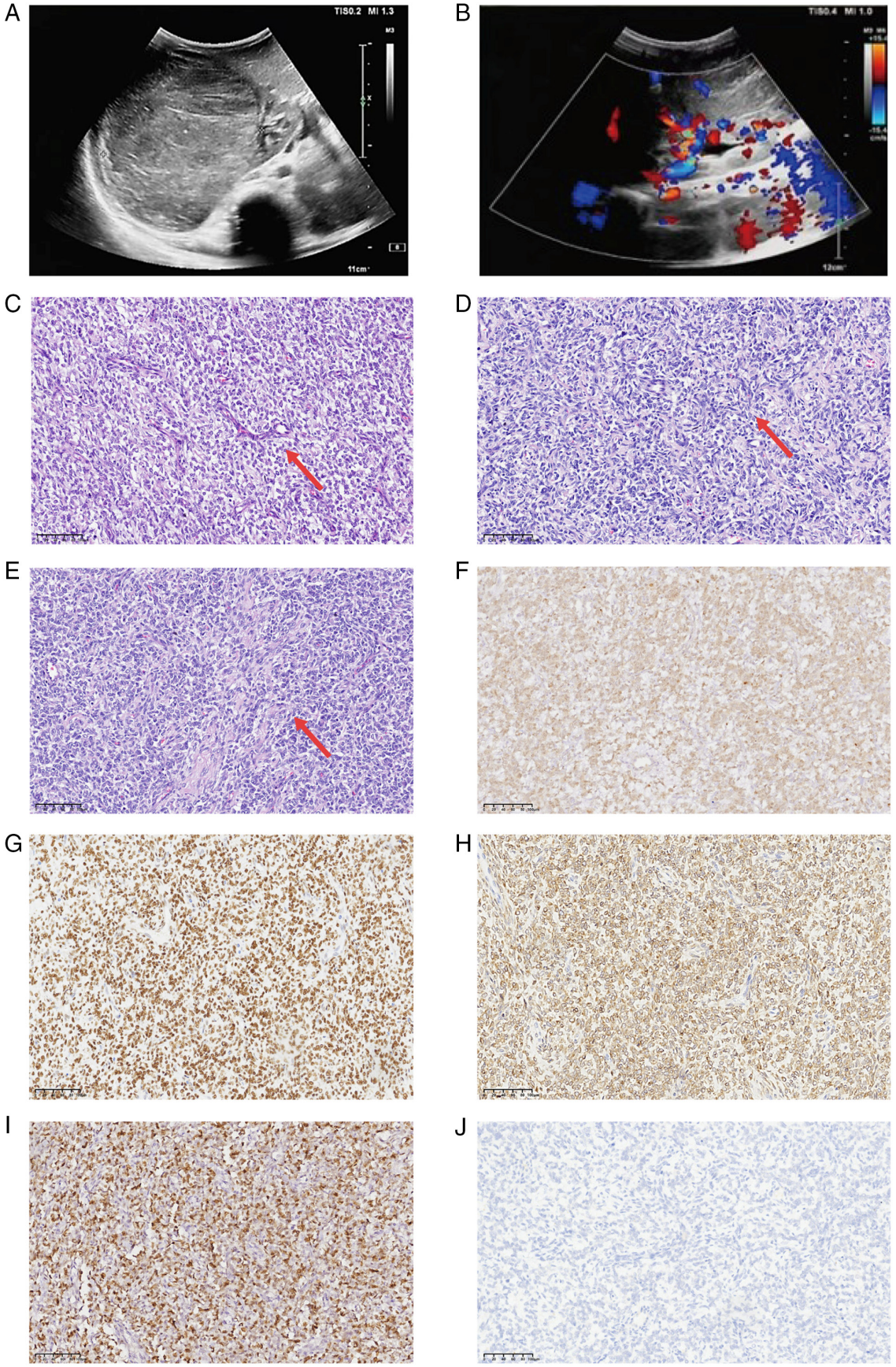

Figure 1. Clinical information of patient 1. (A) Gray-scale ultrasound of the transverse section of the right kidney showed a solid mass occupying the lower-middle part of the kidney, protruding towards the abdominal cavity. (B) Color Doppler flow Imaging shows abundant blood flow signals. Repeated exploration suggested branches of the renal artery extending into CCSK. (C) Patient 1 was diagnosed with classical CCSK. Tumor cells (arrows) are separated by fibrovascular stroma distributed in a dendritic pattern. (D) Tumor cells (arrows) are arranged in a vortex pattern. (E) Patient was diagnosed with classical CCSK. Widened vascular fibrous septa were observed. (F) BCL6 corepressor (positive), (G) transducin-like enhancer of Split 1 (positive), (H) B-cell lymphoma 2 (positive), (I) Cyclin D1 (positive), (J) Wilms' Tumor 1 (negative) immunohistochemistry. Magnification, x20. CCSK, clear cell sarcoma of the kidney.

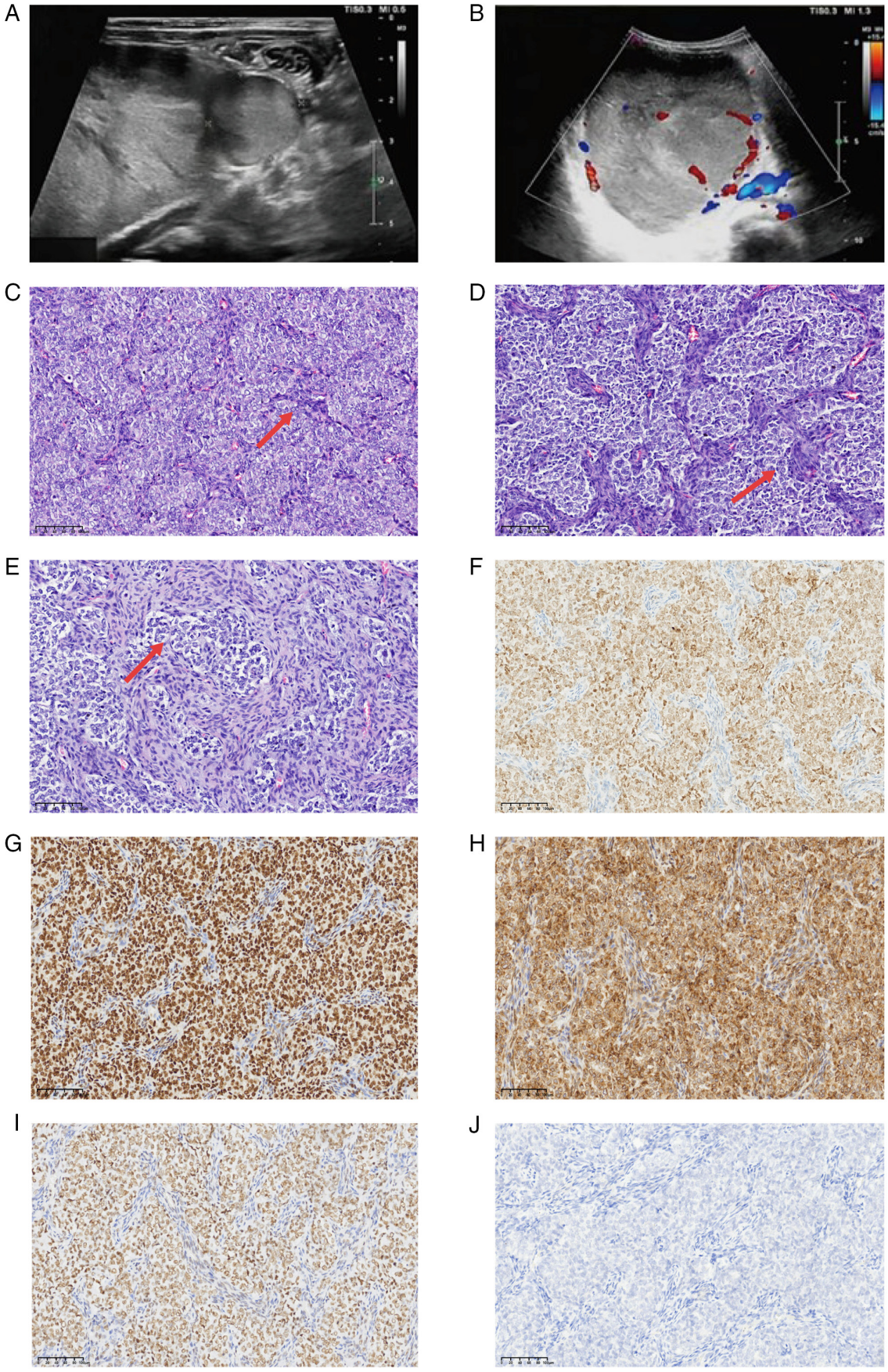

Figure 2. Clinical information of Patient 2. (A) Prone position transverse section imaging showed a solid mass ~9.7x8.5x8.0 cm in size at the middle and lower pole of the right kidney. (B) Color Doppler flow imaging showed rich blood flow signals at the margin. (C) Tumor cells had large nuclei with transparent cytoplasm, and the blood vessels were irregularly distributed. (D) Coarse fibrovascular tissue and sheet-like tumor tissue were observed. (E) Epithelioid tumor cells were arranged in cord-like and small nested patterns. (F) BCL6 corepressor (positive), (G) transducin-Like Enhancer of Split 1 (positive), (H) B-cell lymphoma 2 (positive) (I) Cyclin D1 (positive), (J) Wilms' tumor 1 (negative) immunohistochemistry. Magnification, x20.

without discarding any pellet. One milliliter of xylene had been added again, the tube vortexed, and the centrifugation at 6,000 x g 23˚C for 2 min and supernatant removal repeated. After dewaxing, 1 ml of 96-100% ethanol was added to the pellet and vortexed, followed by centrifugation at 6,000 x g for 2 min; the supernatant had been pipetted off without removing pellet. The tube lid had been opened and incubated at 15-25˚C (or up to 37˚C) for 10 min until residual ethanol evaporated (or dried via vacuum pump). The pellet had been resuspended in 200 μl Buffer GA, 20 μl proteinase K added and vortexed, then incubated at 56˚C for 1 h (until lysis) and 90˚C for 1 h-longer/higher-temperature incubation might have fragmented DNA more, and with one heating block, the sample had been left at room temperature until the block reached 90˚C, with a brief centrifugation to remove lid drops. For RNA-free DNA, 2 μl RNase A (100 mg/ml) was added for 2 min at room-temperature incubation. After lysis, 220 μl Buffer GB had been added and vortexed thoroughly, then 250 μl 96-100% ethanol added and vortexed again, with a brief centrifugation-critical that the mixture was homogeneous. The entire lysate had been carefully transferred to column CR2 (in a 2 ml collection tube) without wetting the rim, centrifuged at 6,000 x g (8,000 rpm) for 2 min, and the column placed in a clean collection tube. Next, 500 μl Buffer GD had been added without wetting the rim, centrifuged at 6,000 x g for 1 min, waste poured out, and the column replaced. Then 500 μl Buffer PW had been added, centrifuged at 6,000 x g for 1 min, waste poured out, and the column replaced again. The column had been centrifuged at full speed (20,000 x g) for 2 min, waste discarded, and the lid opened to dry residual Buffer PW for 2-5 min. Finally, the column had been placed in a clean 1.5 ml tube, 30-100 μl ddH2O applied to the membrane center, left for 2-5 min, centrifuged at full speed for 2 min, and the DNA stored at -20˚C. This result indicated that the BCOR gene had ITD, which was consistent with the pathological diagnosis of CCSK [2].

Tissue wax blocks were cut at a thickness of 7 μm for gene detection. In patient 1, copy number variation in the BCOR gene was detected, with a mutation frequency of 6.47% (Fig. 3A). Moreover, a high frequency of missense mutation in thyroid stimulating hormone receptor (TSHR), which serves a key role in tumor progression, was observed (Fig. 3B). The sequencing results for patient 2 did not reveal definitive BCOR gene mutations, but multiple other gene mutations were present (Fig. 3C and D).

Patient 1 underwent a chemotherapy port implantation procedure, supplemented by nutritional support therapy [central or peripheral venous routes, administer parenteral nutrition preparations (such as glucose, amino acids, fat emulsions, vitamins and minerals, etc.) and was followed for 14 months postoperatively. The right kidney exhibited favorable recovery. Abdominal examination revealed a flat contour without abnormal protrusion or masses. At 1 year after port implantation, clinical evaluation showed no notable abnormality, leading to uneventful port removal with minimal surgical trauma and no postoperative complaints. Follow-up imaging (June 2025) indicated no notable findings in the right renal region, while the left kidney demonstrated normal morphology with intact encapsulation and distinct corticomedullary differentiation (Fig. 4A and B). Patient 2 received intermittent chemotherapy

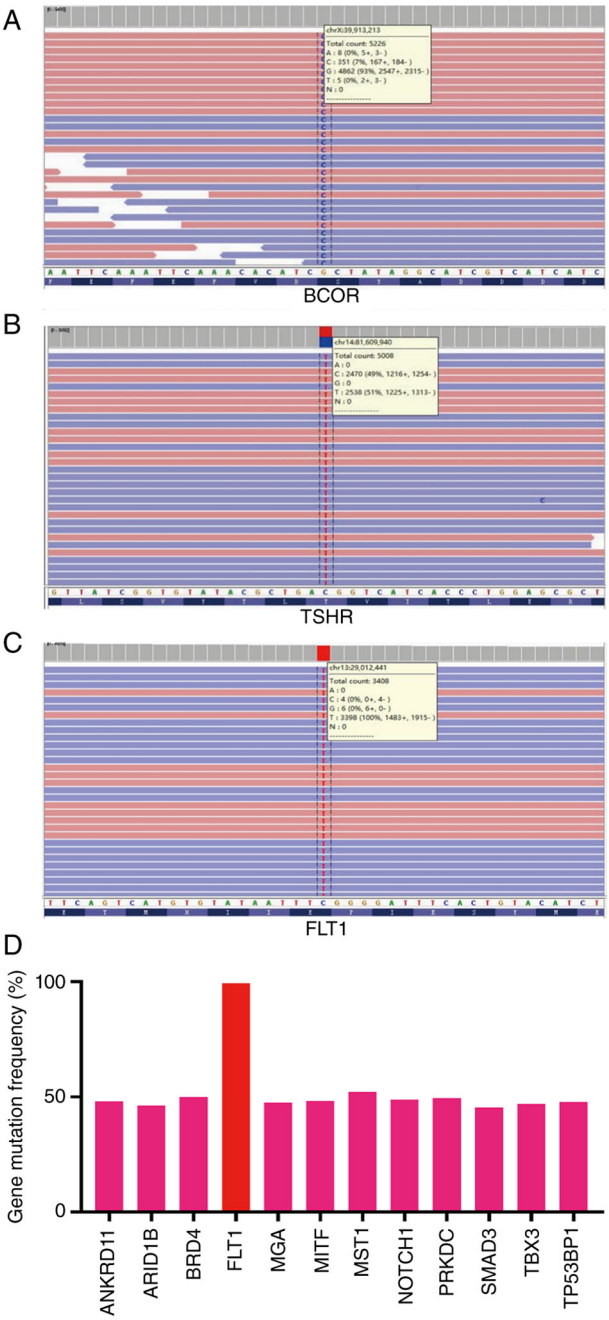

Figure 3. DNA sequencing. Sequencing map of (A) BCOR and (B) TSHR genes in patient 1 tumor tissue. (C) Sequencing map of FLT1 genes in patient 2 tumor tissue. (D) Mutated genes in patient 2. BCOR, BCL6 Co-repressor; TSHR, Thyrotropin Receptor; FLT1, Fms-like Tyrosine Kinase 1; ANKRD, ankyrin Repeat Domain; ARID, AT-Rich Interaction Domain; BRD, Bromodomain-containing; MGA, managing General Agent; MITF, Microphthalmia-Associated Transcription Factor; MST, Mitogen-Activated Protein Kinase Kinase Kinase; NOTCH, Notch Receptor; PRKDC, Protein Kinase, DNA-Activated, Catalytic Polypeptide; SMAD3, SMAD Family Member 3; TBX, T-Box Transcription Factor; TP53BP1, Tumor Protein P53 Binding Protein 1.

(April 2024-June 2025) after surgery. Subsequent upper abdominal ultrasonography revealed no localized masses or sonolucent areas in the right renal region, although splenomegaly was noted (splenic thickness, ~2.7 cm). The left kidney maintained normal size, morphology and echogenicity, with no dilatation observed in bilateral ureters (Fig. 4C and D). In summary, CCSK was

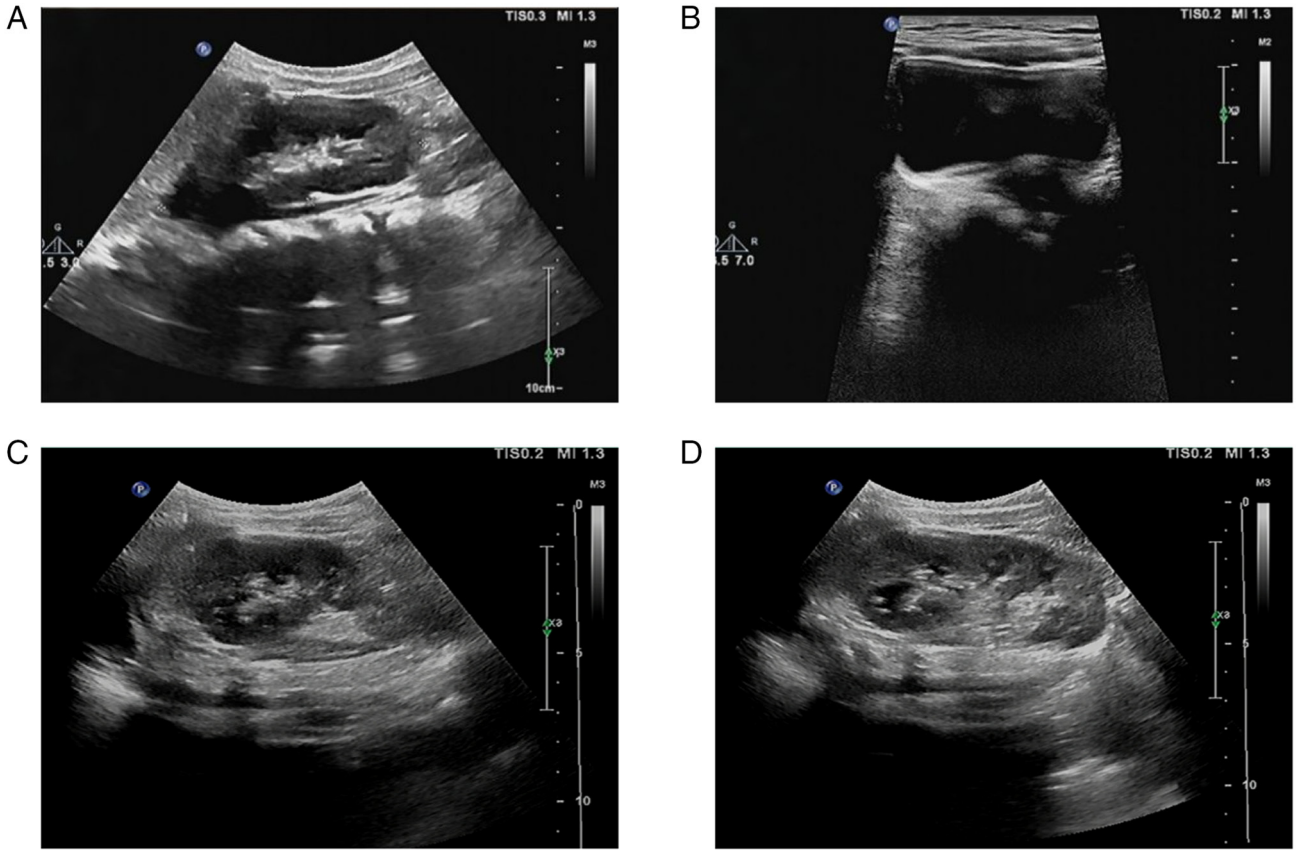

Figure 4. Clinical information of patients 1 year after the surgery. (A) CDFI of patient 1 showed no remarkable findings in the right renal region. (B) while the left kidney demonstrated normal morphology. (C) CDFI of patient 2 showed no localized masses or sonolucent areas in the right renal region, (D) though splenomegaly was noted. CDFI, color Doppler Flow Imaging).

effectively controlled in both pediatric cases, with satisfactory postoperative recovery outcomes. No tumor recurrence was observed as of August 2025.

Patient 1 underwent eight cycles of chemotherapy. The first seven cycles were administered according to the diagnostic and therapeutic recommendations for pediatric WT: Cyclophosphamide (0.52 mg); Actinomycin D (0.47 mg, with a total dose of 3 bottles); Ondansetron hydrochloride (1 mg, with a total dose of 1 vial); 0.9% sodium chloride (50 mg/day), primarily utilizing vincristine-based chemotherapy, during which the patient experienced one seizure. A definitive diagnosis of CCSK was made, and the patient was treated with doxorubicin hydrochloride chemotherapy and had a good mental status. Patient 2 received 27 cycles of chemotherapy, with the treatment regimen continuously adjusted. The patient received multiple courses of vincristine (0.57 mg), cyclophosphamide (the single dose is 23 mg, with a total dose of 3 bottles), etoposide (the single dose is 2 mg, with a total dose of 1 bottles), doxorubicin (1.5 mg/kg) + vincristine (0.05 mg/kg each time, one day), cyclophosphamide (14.7 mg/kg/day x3 days) + etoposide (3.3 mg/kg/day x5 days) and doxorubicin + vincristine + cyclophosphamide, each cycle lasts for 21 days, with a total of 6 to 8 cycles.

Discussion

In 1978, CCSK was recognized as an independent entity (14). Researchers (5-7) have reported that CCSK is characterized by early bone metastasis, which distinguishes it from nephroblastoma. CCSK is a rare and malignant disease that affects infants and young children; however, its pathogenesis remains elusive. The pathological morphology of CCSK (15) is diverse and includes classic, myxoid, cellular, spindle, ring, sclerosing, epithelioid, palisading and anaplastic types, which leads to diagnostic challenges. Moreover, CCSK lacks a distinctive immunophenotype, complicating its morphological and molecular differentiation from nephroblastoma or other pediatric tumors. The present ultrastructural pathological observation of CCSK revealed that the tumor cells had complex projections extending into the surrounding extracellular matrix, which caused vacuolated cytoplasmic artifacts observed under light microscopy. However, the characteristic changes indicative of the origin of tumor cells have not yet been identified. Recent studies have established an association between CCSK and the BCOR gene, which serves as the only marker with high sensitivity and specificity. In clinical practice, CCSK has been accurately diagnosed by the specific nuclear expression of BCOR (16-18), including the two cases reported in the present study. Here, IHC revealed negative expression of WT1, a key molecular marker for diagnosing nephroblastoma, suggesting a potential role involving the expression of BCOR and WT1, aiding the differential diagnosis of these tumors.

Owing to the limited number of cases of CCSK, the molecular mechanisms underlying this condition remain incompletely understood. However, BCOR, tyrosine 3-monooxygenase/tryptophan 5-monooxygenase activation protein ε

(YWHAE), TLE1 and CCND1 serve key roles in the diagnosis of CCSK. These molecules exhibit distinct sensitivity and specificities for CCSK. Notably, BCOR is highly sensitive and specific, making it a key biomarker for the diagnosis of CCSK. BCOR-ITD was identified as the pathogenic mechanism underlying CCSK (19). Distinct ITDs are implicated in specific amino acid regions. In CCSK cases harboring BCOR-ITD, TP53 deletion or mutation is observed and the co-occurrence of both is associated with a poor prognosis in pediatric patients (20). Notably, <75% of CCSK cases exhibit BCOR-ITD fusion (21,22), while a minority demonstrate YWHAE-NUTM2 fusion (22). The detection of YWHAE in CCSK sequencing implies a potential factor associated with maternal inheritance. Additionally, YWHAE promotes the osteogenic differentiation of mesenchymal stem cells and is hypothesized to act via the same pathway as BCOR. TLE1 and CCND1, characterized by relatively low specificity, aid in the differential diagnosis of CCSK (23,24). Moreover, additional molecules have been identified, although their diagnostic performance has not yet been quantitatively validated and should be used in conjunction with other tumor markers (Supplementary Material 1). The present study demonstrated high-frequency expression of the FLT1 gene; to the best of our knowledge, however, there is currently no evidence to confirm a direct association between this gene and the occurrence of CCSK.

Despite the increasing number of reports on specific molecules (19-32), such as BCOR and FLT1 reliable research on the corresponding molecular pathological mechanisms is lacking. Abnormal activation of the MAPK/PI3K/AKT signaling pathway in CCSK currently lacks data to support drug targets and is limited to cell studies, indicating limitations in existing research (23). Research on CCSK focuses mainly on describing preliminary disease characteristics, and a gap remains in the study of its underlying mechanisms. It was hypothesized that several molecular mechanisms may be involved in CCSK, such as abnormal activation of the Wnt pathway due to YWHAE gene fusion or ITD of BCOR, which leads to the upregulation of the downstream target factor CCND1 (33), thereby triggering abnormal cell proliferation and tumorigenesis, or promotion of tumor cell proliferation by YWHAE upregulation via phosphorylation of the PI3K/AKT/Bcl-2 signaling pathway (27-29). However, these hypotheses require validation. The ultrahigh-frequency mutation in FLT1 was noteworthy. In both cases, the children were female and aged 1 year, and there were cases of misdiagnosis of nephroblastoma. Misdiagnoses primarily result from the absence of detailed molecular pathological testing in the initial stages; reliance solely on clinical palpation and imaging diagnostics is insufficient to distinguish this condition from the more common nephroblastoma. With IHC staining and sequencing technologies based on BCOR, an accurate diagnosis was achieved. Both cases showed similar IHC staining features, and in this case, the tumor tissue showed strong and diffuse BCOR nuclear markers. The tumors also showed diffuse immunoreactivity for Bcl2, CD56, cyclin D1 and TLE1 (34). The S100 protein and WT1 results were negative. WT1 expression is important for the diagnosis and differential diagnosis of Wilms' blastoma, whereas positive BCOR expression is evidence for the diagnosis of CCSK.

Overall, conventional chemotherapy has notable side effects [decreased white blood cells, platelets and red blood cells lead to weakened immunity, increased susceptibility to infections, bleeding tendencies (such as nosebleeds, gum bleeding) or anemia (feeling tired, pale complexion).2.Nausea, vomiting, diarrhea, constipation, loss of appetite, oral ulcers.3.Rash, itching, breathing difficulty, low blood pressure.4.Slow growth in height and weight.] when used in pediatric patients, impacting the physical and mental development of children. Hence, identifying the precise targets for CCSK is key. The present study detected high-frequency mutations in TSHR and FLT1. TSHR is involved in regulating thyroid cell metabolism and the process of hereditary pregnancy (35). Aberrant activation of the TSH/TSHR signaling pathway promotes tumor cell immune evasion (36). FLT1 typically regulates the expression of vascular endothelial growth factor and acts via the receptor tyrosine kinase signaling pathway (37). High-frequency mutations in FLT1 are typically associated with abnormally rich blood flow within the tumor and increased activity of sarcoma cells, which are detrimental to prognosis (37). This is also one of the key reasons patient 2 experienced faster tumor progression and poorer prognosis than patient 1. Analysis of the mutated genes in both patients indicated the presence of multiple signaling pathway disorders in CCSK. Other mutated genes did not exhibit stable mutation patterns, indicating notable heterogeneity in CCSK. However, both cases showed positive BCOR expression, consistent with previous literature (15-18). Although only one patient had a BCOR mutation in the gene test, both patients exhibited positive expression via IHC. Therefore, development of targeted therapies that focus on more precise specific molecular targets, such as BCOR-ITD, TCF21 hypermethylation (38) and YWHAE-NUTM2 fusion genes, is feasible. Following diagnosis, the families of patients opted to seek further treatment at higher-tier medical institutions and it was not possible to acquire precise data. Although CCSK is relatively rare, it is essential to develop precision medicine for prognosis prediction and treatment.

Acknowledgements

Not applicable.

Funding

No funding was received.

Availability of data and materials

The data generated in the present study may be found in the Open Science Framework (under accession number 17605) or at the following URL: osf.io/asr2w.

Authors' contributions

HY performed experiments. LL analyzed data and edited the manuscript. HM analyzed and interpreted data. NZ conceived and design. HX interpreted data. LL and HX confirm the authenticity of all the raw data. All authors have read and approved the final manuscript.

Ethics approval and consent to participate

The present study was conducted with ethical approval obtained from the Medical Research Ethics Review Committee of Peking University First Hospital Ningxia Women and Children Hospital (Ningxia Hui Autonomous Region Maternal and Child Health Hospital, Ningxia; China), in accordance with the protocol approved by the ethics committee, adhering to the principles of Good Clinical Practice and the Declaration of Helsinki. The approval number is KJ-LL-2025004. Written informed consent was obtained from the parents/legal guardians of patients aged <18 years.

Patient consent for publication

Not applicable.

Competing interests

The authors declare that they have no competing interests.

References

1. Chen S, Li M, Li R, Cao J, Wu Q, Zhou T, Cai Z and Li N: Clear cell sarcoma of the kidney in children: A clinopathologic analysis of three cases. Int J Clin Exp Pathol 13: 771-777, 2020.
2. Aw SJ and Chang KTE: Clear cell sarcoma of the kidney. Arch Pathol Lab Med 143: 1022-1026, 2019.
3. Gooskens SL, Furtwängler R, Vujanic GM, Dome JS, Graf N and van den Heuvel-Eibrink MM: Clear cell sarcoma of the kidney: A review. Eur J Cancer 48: 2219-2226, 2012.
4. Argani P, Perlman EJ, Breslow NE, Browning NG, Green DM, D'Angio GJ and Beckwith JB: Clear cell sarcoma of the kidney: A review of 351 cases from the national wilms tumor study group pathology center. Am J Surg Pathol 24: 4-18, 2000.
5. Ng A, Jenkinson H, Morland B and Grundy R: Clear cell sarcoma: A dilemma on pathological staging and clinical management. Pediatr Hematol Oncol 22: 257-261, 2005.
6. Kusumakumary P, Mathews A, James FV, Chellam VG, Hariharan S, Varma RR and Nair MK: Clear cell sarcoma kidney: Clinical features and outcome. Pediatr Hematol Oncol 16: 169-174, 1999.
7. Furtwängler R, Gooskens SL, van Tinteren H, de Kraker J, Schleiermacher G, Bergeron C, de Camargo B, Acha T, Godzinski J, Sandstedt B, *et al*: Clear cell sarcomas of the kidney registered on international society of pediatric oncology (SIOP) 93-01 and SIOP 2001 protocols: A report of the SIOP renal tumour study group. Eur J Cancer 49: 3497-3506, 2013.
8. Jackson TJ, Williams RD, Brok J, Chowdhury T, Ronghe M, Powis M, Pritchard-Jones K and Vujanić GM; Children's Cancer and Leukaemia Group (CCLG) Renal Tumours Group: The diagnostic accuracy and clinical utility of pediatric renal tumor biopsy: Report of the UK experience in the SIOP UK WT 2001 trial. Pediatr Blood Cancer 66: e27627, 2019.
9. Friesenbichler W, Lüftinger R, Kropshofer G, Henkel M, Amann G, Furtwängler R, Graf N and Kager L: Clear cell sarcoma of the kidney in Austrian children: Long-term survival after relapse. Pediatr Blood Cancer 68: e28860, 2021.
10. Charafe E, Penault-Llorca F, Mathoulin-Portier MP, Bladou F, Delpéro JR, Prime-Guitton C, Vieillefond A, Xerri L and Hassoun J: Clear cell sarcoma of the kidney relapsing after 10 years of asymptomatic evolution. Ann Pathol 17: 400-402, 1997 (In French).
11. Zhang Y, Chu Q, Ma Y, Miao C and Diao JJ: Overall survival nomogram and relapse-related factors of clear cell sarcoma of the kidney: A study based on published patients. Front Pediatr 10: 943141, 2022.
12. Gooskens SL, Graf N, Furtwängler R, Spreafico F, Bergeron C, Ramírez-Villar GL, Godzinski J, Rübe C, Janssens GO, Vujanic GM, *et al*: Position paper: Rationale for the treatment of children with CCSK in the UMBRELLA SIOP-RTSG 2016 protocol. Nat Rev Urol 15: 309-319, 2018.
13. Astolfi A, Fiore M, Melchionda F, Indio V, Bertuccio SN and Pession A: BCOR involvement in cancer. Epigenomics 11: 835-855, 2019.
14. Morgan E and Kidd JM: Undifferentiated sarcoma of the kidney: A tumor of childhood with histopathologic and clinical characteristics distinct from Wilms' tumor. Cancer 42: 1916-1921, 1978.
15. Drut R and Pomar M: Cytologic characteristics of clear-cell sarcoma of the kidney (CCSK) in fine-needle aspiration biopsy (FNAB): A report of 4 cases. Diagn Cytopathol 7: 611-614, 1991.
16. Fiore M, Taddia A, Indio V, Bertuccio SN, Messelodi D, Serravalle S, Bandini J, Spreafico F, Perotti D, Collini P, *et al*: Molecular signature of biological aggressiveness in clear cell sarcoma of the kidney (CCSK). Int J Mol Sci 24: 3743, 2023.
17. Wong MK, Ng CCY, Kuick CH, Aw SJ, Rajasegaran V, Lim JQ, Sudhanshi J, Loh E, Yin M, Ma J, *et al*: Clear cell sarcomas of the kidney are characterised by BCOR gene abnormalities, including exon 15 internal tandem duplications and BCOR-CCNB3 gene fusion. Histopathology 72: 320-329, 2018.
18. Kao YC, Sung YS, Zhang L, Huang SC, Argani P, Chung CT, Graf NS, Wright DC, Kellie SJ, Agaram NP, *et al*: Recurrent BCOR internal tandem duplication and YWHAE-NUTM2B fusions in soft tissue undifferentiated round cell sarcoma of infancy: Overlapping genetic features with clear cell sarcoma of kidney. Am J Surg Pathol 40: 1009-1020, 2016.
19. Ueno-Yokohata H, Okita H, Nakasato K, Akimoto S, Hata J, Koshinaga T, Fukuzawa M and Kiyokawa N: Consistent in-frame internal tandem duplications of BCOR characterize clear cell sarcoma of the kidney. Nat Genet 47: 861-863, 2015
20. Singh V, Gupta K, Saraswati A, Peters NJ and Trehan A: Role of cyclin D1 and BCOR immunohistochemistry in differentiating clear cell sarcoma of kidney from its mimics. J Pediatr Hematol Oncol 43: 294-300, 2021.
21. Zhang M, Yao X, Guan X, Jia C, Zhang R, Wang H, Guo Y, Ni X, Yu Y and He L: Clinical relevance of BCOR internal tandem duplication and TP53 aberration in clear cell sarcoma of the kidney. Hum Pathol 134: 45-55, 2023.
22. Kenny C, Bausenwein S, Lazaro A, Furtwängler R, Gooskens SL, van den Heuvel Eibrink M, Vokuhl C, Leuschner I, Graf N, Gessler M and O'Sullivan MJ: Mutually exclusive BCOR internal tandem duplications and YWHAE-NUTM2 fusions in clear cell sarcoma of kidney: Not the full story. J Pathol 238: 617-620, 2016.
23. Li X, Wang C, Wang S, Hu Y, Jin S, Liu O, Gou R, Nie X, Liu J and Lin B: YWHAE as an HE4 interacting protein can influence the malignant behaviour of ovarian cancer by regulating the PI3K/AKT and MAPK pathways. Cancer Cell Int 21: 302, 2021.
24. Yang YF, Lee YC, Wang YY, Wang CH, Hou MF and Yuan SF: YWHAE promotes proliferation, metastasis, and chemoresistance in breast cancer cells. Kaohsiung J Med Sci 35: 408-416, 2019.
25. Zhao J, Xu H, Duan Z, Chen X, Ao Z, Chen Y, Ruan Y and Ni M: miR-31-5p regulates 14-3-3 ε to inhibit prostate cancer 22RV1 cell survival and proliferation via PI3K/AKT/Bcl-2 signaling pathway. Cancer Manag Res 12: 6679-6694, 2020.
26. Yan L, Gu H, Li J, Xu M, Liu T, Shen Y, Chen B and Zhang G: RKIP and 14-3-3ε exert an opposite effect on human gastric cancer cells SGC7901 by regulating the ERK/MAPK pathway differently. Dig Dis Sci 58: 389-396, 2013.
27. Gooskens SL, Kenny C, Lazaro A, O'Meara E, van Tinteren H, Spreafico F, Vujanic G, Leuschner I, Coulomb-L'Herminé A, Perotti D, *et al*: The clinical phenotype of YWHAE-NUTM2B/E positive pediatric clear cell sarcoma of the kidney. Genes Chromosomes Cancer 55: 143-147, 2016.
28. Kenny C, McDonagh N, Lazaro A, O'Meara E, Klinger R, O'Connor D, Roche F, Hokamp K and O'Sullivan MJ: Dysregulated mitogen-activated protein kinase signalling as an oncogenic basis for clear cell sarcoma of the kidney. J Pathol 244: 334-345, 2018.
29. Ali Z, Haroon Khan A, Rehman U, Faisal M, Ahmad IN, Mamoon N, Nasir H and Hameed Z: Is TLE1 expression limited to synovial sarcoma? Our experience at Shifa International Hospital, Pakistan. Cureus 11: e6259, 2019.
30. Bergeron BP, Barnett KR, Bhattarai KR, Mobley RJ, Hansen BS, Brown A, Kodali K, High AA, Jeha S, Pui CH, *et al*: Mutual antagonism between glucocorticoid and canonical Wnt signaling pathways in B-cell acute lymphoblastic leukemia. Blood Adv 7: 4107-4111, 2023.
31. Hasbay B and kayaselCuk F: Expression of TLE-1 in gastrointestinal stromal tumour and its relationship to clinicopathological parameters. J Coll Physicians Surg Pak 33: 286-291, 2023.

32. Milman T, Eiger-Moscovich M, Henry RK, Ida CM, Ruben M, Shields CL, Lally SE, Penne RB, Stefanyszyn MA, Bilyk JR, *et al*: Cyclin D1 expression and molecular genetic findings in periocular histiocytoses and neoplasms of macrophage-dendritic cell lineage. Am J Ophthalmol 242: 36-51, 2022.
33. Mirkovic J, Calicchio M, Fletcher CD and Perez-Atayde AR: Diffuse and strong cyclin D1 immunoreactivity in clear cell sarcoma of the kidney. Histopathology 67: 306-312, 2015.
34. Uddin N, Minhas K, Abdul-Ghafar J, Ahmed A and Ahmad Z: Expression of cyclin D1 in clear cell sarcoma of kidney. Is it useful in differentiating it from its histological mimics? Diagn Pathol 14: 13, 2019.
35. Narumi S, Muroya K, Abe Y, Yasui M, Asakura Y, Adachi M and Hasegawa T: TSHR mutations as a cause of congenital hypothyroidism in Japan: A population-based genetic epidemiology study. J Clin Endocrinol Metab 94: 1317-1323, 2009.
36. Wu Z, Xi Z, Xiao Y, Zhao X, Li J, Feng N, Hu L, Zheng R, Zhang N, Wang S and Huang T: TSH-TSHR axis promotes tumor immune evasion. J Immunother Cancer 10: e004049, 2022.
37. Muetze S, Kapagerof A, Vlachopoulos L, Eggermann T, Kaufmann P, Zerres K, Rath W and Rudnik-Schoeneborn S: Mutation analysis of the growth factor genes PlGF, Flt1, IGF-I, and IGF-IR in intrauterine growth restriction with abnormal placental blood flow. J Matern Fetal Neonatal Med 23: 142-147, 2010.
38. Sazonova O, Zhao Y, Nürnberg S, Miller C, Pjanic M, Castano VG, Kim JB, Salfati EL, Kundaje AB, Bejerano G, *et al*: Characterization of TCF21 downstream target regions identifies a transcriptional network linking multiple independent coronary artery disease loci. PLoS Genet 11: e1005202, 2015.